DESIGN AND EXPERIMENTAL STUDY OF HIGH-EFFICIENCY AND LOW-DAMAGE BIONIC PICKING DEVICE FOR TOBACCO LEAVES
/
高效低损伤烟叶仿生采摘装置的设计与试验研究

Chenhui ZHU[1)], Bingjie CHEN[1)], Bo LUO[1, 3)], Wanzhang WANG[1)], Bingjie LIU[4)], Baoshan WANG[1)], Liquan YANG*[1, 2)]

[1)] School of Mechanical and Electrical Engineering, Henan Agricultural University, Zhengzhou 450002, China;
[2)] Henan Province Engineering Research Center of Ultrasonic Technology Application, Pingdingshan University, Pingdingshan 467000, China;
[3)] School of Intelligent Engineering, Zhengzhou College of Finance and Economics, Zhengzhou 450000, China;
[4)] College of Information and Management Science, Henan Agricultural University, Zhengzhou 450002, China
Corresponding author: Liquan YANG
Tel: +8615038352581; E-mail: 2695@pdsu.edu.cn
DOI: https://doi.org/10.35633/inmateh-75-84

Keywords: *agricultural machinery, tobacco leaf picking, bionic, low damage*

ABSTRACT
To address the issues of high damage rate and low harvesting efficiency during the tobacco leaf picking process, this study analyzed the separation mechanics of tobacco stems and leaves. A low-damage bionic picking device was designed by imitating the manual method of harvesting tobacco leaves. Based on theoretical analysis of the device and its key components, the structure and parameters of the complete system were determined. The picking process was simulated using ADAMS software, focusing on the contact force between the rigid and flexible components at various picking rod speeds. This analysis yielded the optimal combination of structural and operational parameters. Field experiments were subsequently conducted, and a response surface mathematical model was established using Design-Expert software to evaluate the relationship between key factors and performance indicators. The optimal parameter combination was found to be: a picking rod speed of 0.8 m/s, a device inclination angle of 30°, a picking rod spacing of 90 mm, and a forward speed of 0.69 m/s. Under these conditions, the tobacco leaf damage rate was minimized, meeting the requirements for low-damage harvesting. Further experimental validation showed consistency with simulation results, confirming the model's reliability and demonstrating the practical feasibility of the device for tobacco field operations. This provides a valuable reference for the development of low-damage tobacco leaf harvesting equipment.

摘要
为解决目前烟叶采摘装置在采收过程中烟叶破损率高、采净率低的问题，对烟叶的茎叶分离进行分析，模仿人手采摘烟叶方式，设计了一种低损伤烟叶仿生采摘装置。通过对该装置及关键部位的理论分析，确定整体装置的结构和参数。利用 ADAMS 软件对烟叶采摘过程进行仿真，分析不同采摘手速度和茎秆送料速度下刚性结构与柔性缓冲结构之间的接触力，得到了最佳参数组合。最后进行了田间试验，使用 Design-Expert 软件，建立各因素与指标的响应面数学模型，分析了各因素与评价指标之间的关系，得到参数优化组合，采摘杆转速为 0.8m/s，装置倾斜角为 30°，采摘指间距为 90mm，前进速度为 0.69m/s，该组合下烟叶破损率最低，满足低损伤采摘的条件。结果基本与仿真结果一致，证明了模型的可靠性。最后进行了田间试验，试验结果表明此装置在实际烟叶田间采摘工作的可行性，为低损伤烟叶收获装置的研发提供了参考。

INTRODUCTION
In the tobacco harvesting process, picking is the most fundamental and challenging operation. The quality of harvested tobacco leaves directly influences the effectiveness of post-harvest grading. As the core component of the harvesting machinery, the picking device plays a crucial role. Therefore, the design of the tobacco leaf picking device is key to ensuring high-quality tobacco leaf harvesting.

[1] *Chenhui ZHU, Ph.D. Eng.; Bingjie CHEN, M.S. Stud. Eng.; Wanzhang WANG, Prof. Ph.D. Eng.; Baoshan WANG, Ph.D. Eng. Liquan YANG, Associate Prof. Ph.D. Eng.; Bo LUO, Ph.D. Stud.;* [4] *Bingjie LIU, Ph.D. Eng.*

Early tobacco leaf harvesting devices have been categorized into three primary types (*Papusha S.K, 2022*). The first type, a serrated harvesting device, employs a saw-toothed blade to sever the entire tobacco stalk at its base, achieving high operational efficiency. The second type, a chain-and-hole harvesting device, incorporates a series of spaced chains with apertures sized to accommodate the stalk diameter. During operation, the stalk is guided through these apertures, thereby completing the detachment process. Both serrated and chain-and-hole methods are exclusively suitable for fully matured tobacco plants. The third and most widely utilized type is the mechanical striking harvester, which induces leaf detachment by applying downward force on the petiole through controlled mechanical impact. Although these methods demonstrate operational efficiency, they exhibit elevated leaf damage rates (12–18%) and variable collection efficiency (67–82% across field trials). Further design refinements are therefore required to mitigate these limitations, particularly through enhanced stalk-gripping mechanisms and impact force modulation.

With the continuous advancement of modern agricultural technology, the mechanization and intelligentization of tobacco harvesting have become inevitable trends to enhance production efficiency and quality. In recent years, significant achievements have been made by scholars both domestically and internationally in the field of tobacco harvesting machinery and intelligent recognition. *Sun C. (2024)* and colleagues designed and tested key components of a comb-type tobacco harvester, providing valuable insights for optimizing tobacco harvesting equipment. *Liu J. (2012)* and *Yu J. (2019)* leveraged virtual manufacturing technology to design and simulate a tobacco harvesting system, further advancing the intelligence and automation of harvesting processes. *Zhu H. (2014)* developed a floating harvesting platform based on the advantages and disadvantages of tobacco leaf harvesting processes. This platform enables selective harvesting by determining the relative position of leaves and the harvesting device using sensor rods, while hydraulic systems control the platform's lateral movement and elevation. *Gan W. (2018)* and colleagues designed a tobacco leaf harvesting device featuring left and right curved blades connected via a rotating axis. This design effectively harvests mature leaves while protecting unripe ones, ensuring efficient and low-damage harvesting.

Bionic picking machinery is designed and improved by studying biological mechanisms and imitating the shape, structure, or function of organisms. Currently, bionic mechanical design has been widely applied in fields such as sensors and new materials, with numerous studies (Luo, Y. et al., 2024.) published in this area. Beyond developing cutting end effectors with low cutting resistance, bionic optimization of these effectors is achieved by mimicking the fingers and claws of natural organisms. Research in this field primarily focuses on crops such as fruits (*Malekzadeh, 2019; He Z., 2022; Kurbah F., 2022*), tea (*Kurbah F., 2022; Nie Y.C., 2022*) and vegetables (*Du Z., 2021*), with tomatoes (*Gao J. et al., 2022; Gao J. et al., 2024; Guo T. et al., 2022; Hou Z. et al., 2021; Wang M. et al., 2022; Zhao L. et al., 2012*) being the most extensively studied. For high-stalk crops like corn and tobacco, scholars have conducted significant research on bionic ear-breaking mechanisms for corn (*Xu W.T. et al., 2018; Zhang L.P. et al., 2015*). A notable example is the work of Zhang Liping and Chen Meizhou *(Zhang L.P. et al., 2015. Chen M.Z. et al., 2018*), who addressed issues such as high impurity rates in plate-type ear picking, gnawing in roller-type ear picking, and significant grain loss. They proposed a bionic ear-breaking hand-type mechanism for corn harvesting, providing valuable insights for the development of low-damage corn harvesting techniques. In contrast, research on bionic picking for tobacco leaves remains limited. *Li Zhiguang (2016)* designed a self-propelled intelligent bionic picking system for tobacco leaves. This system mimics the entire process of manual tobacco harvesting by controlling a bionic picking hand to perform actions such as extending, grasping, picking, releasing, and retracting, thereby reducing damage to both tobacco leaves and stems.

On the basis of drawing lessons from the existing automatic picking machinery of tobacco leaves and other crops, this paper intends to combine modern bionic technology, imitate the action of human hand picking, and apply force to tobacco leaves from top to bottom to make tobacco leaves fall. This paper verifies the possibility of low-loss harvesting of this bionic picking method, which can solve the problems of high crushing rate and low picking rate in the process of automatic picking of tobacco leaves, in order to provide theoretical basis and technical basis for low-damage automatic tobacco leaf picking technology.

ANALYSIS OF THE MANUAL HARVESTING PROCESS AND DESIGN OF BIONIC STRUCTURES

Analysis of Manual Harvesting Actions

Stem-leaf separation constitutes the initial critical stage in flue-cured tobacco harvesting. During mechanized operations, this process exhibits complex mechanical stress distributions due to heterogeneous stalk-foliage interactions.

Such dynamic force conditions frequently induce mechanical injuries to leaves, including surface abrasions, midrib fractures, and lamina tearing, as documented in field studies. Consequently, minimizing mechanical damage rates during automated stem-leaf separation has emerged as a pivotal technical challenge that must be resolved to enable fully mechanized tobacco production systems.

This paper analyzes the motion of manual tobacco leaf harvesting and designs a bionic harvesting device to achieve the purpose of reducing damage and increasing efficiency. Manual harvesting typically involves using the thumb and index finger (the "tiger mouth" position) to grip the leaf stem, pressing straight down until the leaf detaches from the stalk. The following Figure 1 is the manual harvesting process and the force diagram of tobacco leaves.

(**a**) (**b**)

Fig. 1 - Manual harvesting action and force diagram of tobacco leaves

(a) Artificial harvesting method; (b) Harvesting force diagram.

Bionic Design Principles

The crucial part of the bionic tobacco leaf harvesting machine is the bionic picking rod, which acts as the executive mechanism to directly sever the leaves from the stem. The stability of the picking rod's operation directly impacts the performance of the harvester and the quality of the picked tobacco leaves. This study designs the bionic picking rod by mimicking the action of human fingers when picking tobacco leaves, considering that tobacco leaves grow in various directions around the stalk during their growth in the field. Auxiliary rods are therefore positioned vertically along the picking rod, and the two picking rods, in conjunction with the auxiliary rod, form a picking frame that ensures all leaves can be collected. The following Figure 2 is a bionic design.

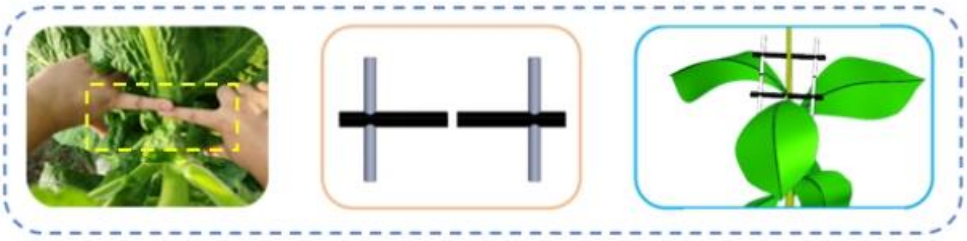

Fig. 2 - Bionic picking principle diagram

Design and Working Principle of Bionic Tobacco Leaf Harvesting Structure

The low-damage bionic tobacco leaf harvesting machine is structured vertically with a collection box at the top, followed by a transmission section, and a harvesting unit at the bottom, as shown in Figure 3. The harvesting unit consists of two oppositely positioned harvesting modules, with a gap reserved between them. The height and tilt angle of the harvesting unit are adjustable to accommodate tobacco plants of varying heights. The transmission section includes a series of rollers positioned below the harvesting unit and a conveyor belt that transports harvested leaves upward toward the collection box. The divider, designed in a triangular conical shape, is mounted at the front of the harvesting mechanism and positioned between two parallel bionic harvesting units, serving as the leading component of the entire apparatus.

This design can complete the layered mechanized picking of tobacco leaves, with low breakage rate and high harvesting efficiency. At the same time, it can greatly reduce the damage to tobacco plants and ensure the normal growth of tobacco plants in the future.

Fig. 3 - The overall structure of tobacco leaf harvester

Working Principle

When the tobacco leaf picking machine starts to harvest tobacco leaves, the tobacco plants are first introduced by the upper and lower pairs of dividers at the front end, and then the tobacco plants enter the bionic picking frame composed of picking rods and auxiliary rods on both sides. The picking frame is fixed on the chain and rotates around the picking frames on both sides, and the back end of the chain plane is tilted downward to ensure that the tobacco leaves within the preset height range can be harvested. The picking frame rotates downward and backward, and the picking machine moves forward. The petiole is subjected to a downward force. When the force is greater than the connection force between the tobacco leaf and the stem, the petiole breaks. After the tobacco leaves are removed, they fall on the conveyor belt below and are then transmitted to the collection box. The picking machine continues to move forward, and the flexible picking rod contacts and bends with the tobacco rod. The tobacco rod enters the next picking frame and carries out the tobacco leaf picking at the next height until the tobacco plant passes through all the picking frames to complete the tobacco leaf picking in the preset height range. The harvesting operation of the whole device imitates the action of rolling tobacco leaves down along the stem during manual picking through the motion synthesis of the picking frame and the whole machine, so as to realize the low-loss picking of tobacco leaves. The schematic diagram of the harvesting process is shown in Figure 4.

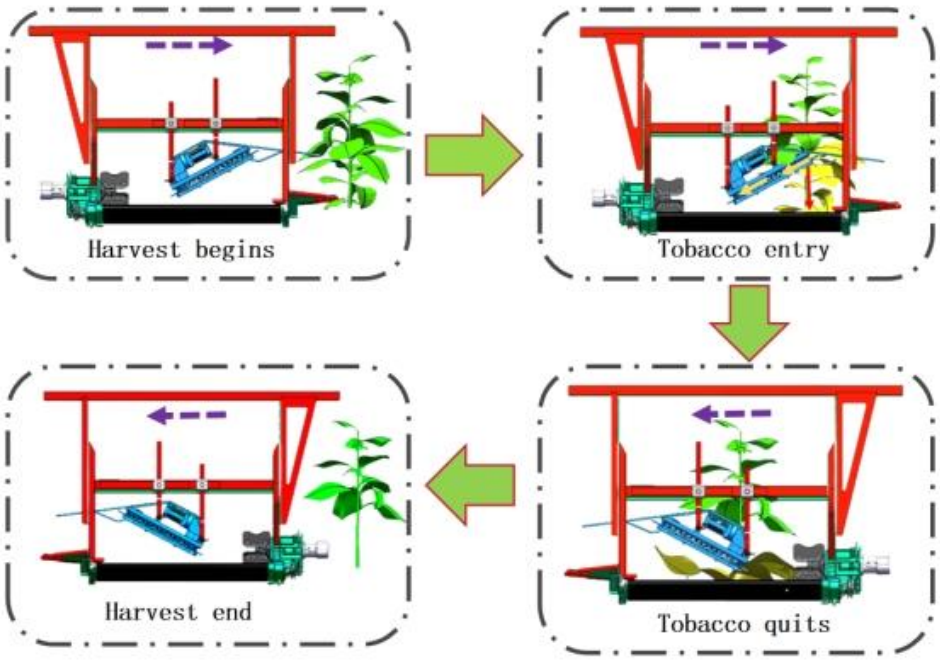

Fig. 4 - Tobacco leaf harvesting process

Analysis of Mechanical Properties in Tobacco Leaf Harvesting Process

Characteristics of Tobacco Leaf Harvesting

The growth characteristics of tobacco leaves and the connection strength of stems and leaves are important basis for the design of bionic picking device. The experiment was conducted in the tobacco fields of Xiangcheng County, Henan Province. The height of tobacco plant is moderate, the oil of tobacco leaf is large, the toughness is good, and it is suitable for mechanized harvesting. As shown in Figure 5, 20 tobacco plants were randomly selected as test objects, and steel ruler, electronic tension meter and protractor were used to measure the trait characteristics of tobacco leaves, the angle between petiole and stem, the position of picking force and the fracture force between stem and petiole. After removing extreme data, the average value of the measurement results was taken: length 58 cm, width 34 cm, stem diameter 3.6 cm, stem leaf angle 46°, petiole fracture force 34 N, which provided data support for the design of bionic picking device.

Fig. 5 - Measurement of tobacco leaf characteristics

Analysis of the Collision Process in Tobacco Leaf Harvesting

In the process of tobacco leaf picking, the collision between the picking device and the tobacco leaf will produce a large impact force. Assuming that the external force impulse is constant, the length of the collision time Δ t will seriously affect the peak impact force. Prolonging the collision time can reduce the collision impact force, thereby reducing the damage rate of tobacco leaves. The tobacco leaf is regarded as a particle, and its collision process conforms to the impulse-momentum theorem:

$$I = \int_{t_0}^{t_0+\Delta t} ma(t)dt \tag{1}$$

Where: I is the impulse of tobacco leaves, N·s; m is the quality of tobacco leaves, kg; a is acceleration, m/s^2; t is time, s.

It can be seen from Equation (1) that the impulse of tobacco leaves during picking is not only related to its own weight, but also affected by collision time and collision acceleration.

Let y be the coordinate of the middle part of the tobacco leaf in the vertical direction, then the motion equation of the single degree of freedom system is:

$$\begin{gathered} m\ddot{y}+c\dot{y}+(k+k_o)y=0 \\ y(0)=0, \dot{y}(0)=v_0 \end{gathered} \tag{2}$$

In the case of underdamping, the solution of Equation (2) is:

$$y = Ae^{-\lambda\omega_i t}\sin\omega_s t \tag{3}$$

where**:**

$$\lambda = \frac{c}{2m\omega_i} \tag{4}$$

$$A = \frac{v_0}{\omega_s} \tag{5}$$

$$\omega_s = \sqrt{1-\lambda^2\omega_i} \tag{6}$$

$$\omega_i = \sqrt{\frac{k+k_0}{m}} \tag{7}$$

In the formula, λ is viscous damping ratio, λ <1; A is amplitude, mm; ω_s is damped natural frequency, Hz; ω_i is undamped natural frequency, Hz.

With an initial displacement of 0, the collision time is determined by the smallest positive root of Eq. (8):

$$f(t) = c\dot{y} + ky = 0 \tag{8}$$

The available collision time is:

$$\Delta t = \frac{\pi + \arctan \lambda_2}{\omega_i \sqrt{1-\lambda^2}} \tag{9}$$

It can be seen from Equation (9) that the impact time is related to the tobacco leaves mass, picking mechanism stiffness coefficient, damping coefficient, and other parameters of the system, and these inherent parameters depend on its structure and materials.

As mentioned above, in the design of the next bionic picking device, the stiffness coefficient can be reduced and the damping coefficient can be increased by changing the structure and contact material of the picking mechanism, thereby reducing the collision acceleration, reducing the impact force at the moment of collision, and finally reducing the damage rate of tobacco leaves.

Bionic Harvesting Device Parameter Design

Harvesting Rod Parameter Design

The bionic picking rod and the auxiliary rod are fixed on the chain, and the chain and the motor are installed on both sides of the frame. The two chains are driven by the motor to rotate around the two sides of the frame. In the process of field operation, as the picking machine moves forward, the tobacco stem enters the picking frame composed of picking rod and auxiliary rod through the guidance of the front divider, as shown in the following Figure 6.

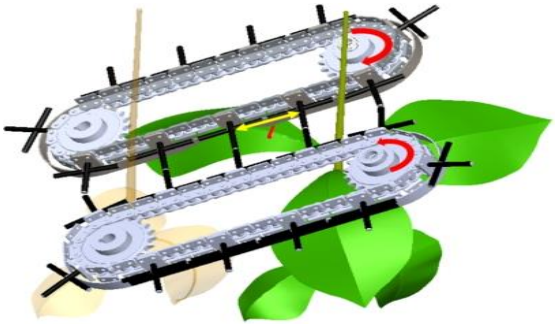

Fig. 6 - Picking rod structure diagram

If the picking frame is set too small, the stem pass ability is reduced, which is likely to cause damage to the stem and seriously affecting the picking effect; if the picking frame is too large, the torque of the tobacco leaves increases, and completing the picking operation requires greater force, resulting in an increase in the power consumption of the picking machine. Secondly, if the picking frame is too large, it will lead to the contact being not with the petiole but with the more fragile blade, resulting in an increase in the picking damage rate. Through field experiments, it has been determined that the distance between two adjacent picking rods on the same side of the transmission chain needs to be optimized:

$$l \times cos\alpha = l_0 + d \tag{10}$$

where, l is the distance between the two picking rods in the same side, mm; α is the angle between the plane and the horizontal plane of picking rod, °; d is diameter, mm; l_0 is tobacco leaf picking position to the distance from the stem pole, mm.

According to the previous measurement and statistics of tobacco stems, d is 35 mm, the angle between the plane of the picking rod and the horizontal plane is 30, and the picking force of the tobacco petiole is tested. The distance from the picking force position to the stem is 70 mm, and it is reasonable to take 92 mm by calculation.

Harvesting Rod Rotation Speed Design

The picking rod rotates with the chain around the frame. It can be seen from the previous calculation that the greater the instantaneous speed of contact between the picking rod and the blade, the greater the impact force on the tobacco leaf, so the excessive speed of the chain will cause the damage rate of the tobacco leaf to increase. If the chain speed is simply reduced, the tobacco stem bent by the picking frame will cause damage to the tobacco stem because it does not pass through the flexible picking frame in time. According to the design principle of the picking device and the agronomic requirements of the layered picking of tobacco leaves, as shown in Figure 7, the speed of the picking frame needs to match the speed of the picking machine to achieve the expected effect of the picking rod relative to the downward movement of the tobacco stem. The speed of the two needs to meet:

$$v_1 = k\frac{v}{\cos\alpha} \tag{11}$$

where, v is picking machine forward operating speed, m/s; k is empirical coefficient; v_1 is the chain rotation speed of picking rod, m/s; α is the angle between the picking mechanism and the horizontal plane, °.

After many field experiments, the value of the empirical coefficient k is 1.0-1.1, the picking frame plane and the horizontal plane are 25°-35°, the integrity of the tobacco leaf is high, the damage to the tobacco stem is low, and the expected operation effect can be better realized. At the same time, in order to ensure the harvest efficiency of 1 to 1.3333 hectares per day, the operating speed v of the tobacco picking machine in the field is 1.5 km/h-4 km/h. When the angle α between the plane of the picking mechanism and the horizontal plane is set to 30°, substituting this value into Equation (11) yields a calculated range for the chain rotation speed v_1 of the picking rod between 0.48 m/s and 1.28 m/s.

Fig. 7 - Velocity relation diagram

Design of Grain Divider

The divider, as the core front-end component of the harvester, primarily serves to upright fallen tobacco plants and guide them into the harvesting mechanism while separating upper and lower leaves to prevent damage during harvesting. Its simple yet critical design directly impacts overall harvesting performance. Featuring symmetrical triangular-cone structures, the divider's effectiveness depends on its angle (β) and front height (l_1). Based on field data, it is designed to handle plants with up to 20° of lodging. For example, in central Henan, where mid-stem leaves grow 0.5–0.9 meters above ground, the front height (l_1) is calculated using the formula:

$$l_1 = 0.9\cos\gamma \tag{12}$$

where, l_1 is the height of the front end of the layered device from the ground, cm; γ is tobacco lodging angle, °, γ = 0~20°.

Because the maturity of tobacco leaves is from bottom to top, the design of the divider only considers the uppermost part of the picking layer. The distance from the front end of the divider to the ground is 84.5 ~ 90 cm, and the inclination angle of the divider should be satisfied.

$$\beta = \arcsin\frac{l_2 - l_1}{l_3} \tag{13}$$

where, β is angle of inclination of the divider, °; l_2 is the height from the rear end of the divider to the ground, cm; l_3 is length of divider, cm.

Through the comprehensive analysis of the characteristics of tobacco field planting in Henan and the agronomic requirements of picking, combined with the design experience, the distance from the front end of the divider to the mechanism is determined to be 46.5 cm, and the height from the connection position of the divider and the mechanism to the ground is 100 cm.

The data is brought into the formula (13) to calculate and sort out the value range of the inclination angle of the divider is about 12.4° ~ 20.7°. The smaller the inclination angle of the divider, the better the effect of the divider and the passing ability. Considering that the picking machine needs to adapt to different heights of tobacco leaves, in order to ensure the picking effect, the inclination angle of the divider should be smaller on the basis of calculation. In summary, the inclination angle of the divider is 10°.

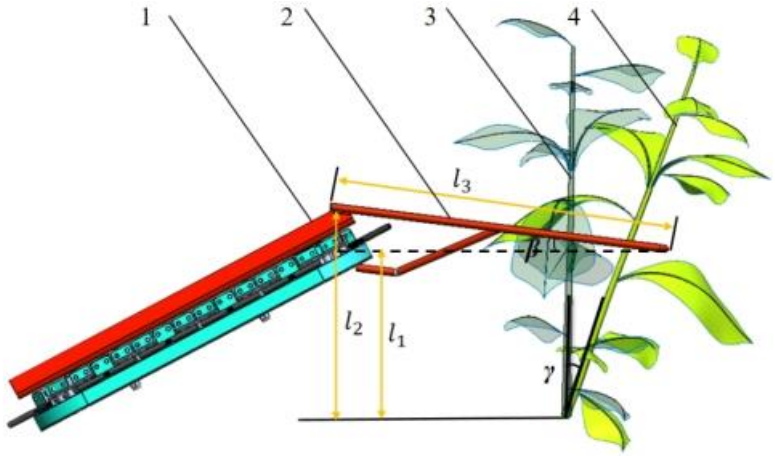

Fig. 8 - Schematic diagram of the staged righting process for lodged tobacco plants

(1) plucking device; (2) division mechanism; (3) uprighted tobacco; (4) lodged tobacco

Tobacco Harvest Simulation

Model Establishment

Based on field measurements of tobacco plant dimensions, the stalk height is set to 1700 mm, the stalk diameter to 4 mm, and the overall leaf dimensions to 600 × 350 mm. A thin-shell structure is created based on the leaf shape. As shown in Figure 9(a), a tobacco plant model is established using SolidWorks software. To clearly illustrate the harvesting process, the plant model is simplified, as shown in Figure 9(b). The simplified model consists of two components: the stalk and the leaf. The leaf is positioned 1000 mm above the ground, and the angle between the leaf stalk and the plant stalk is 50°.

(**a**) (**b**)

(a) Tobacco plant model *(b) Simplified tobacco plant model*

Fig. 9 - Whole tobacco and simplified model

Analysis of Tobacco Leaf Dropping Conditions

By applying an external force to the tobacco leaf, the change of the flexible connection force between the tobacco leaf and the tobacco stem under different forces is analyzed, so as to determine the condition of the

tobacco leaf falling from the tobacco plant, and lay the foundation for the simulation of the next tobacco leaf picking process.

Simulation Parameter Settings

The simplified tobacco plant model built in SolidWorks is imported into ADAMS. The file format is "Parasolid" format, which is relatively stable after conversion and is not easy to lose graphic information. Because the materials provided by the system do not meet the actual needs, the actual tobacco plant materials are created by inputting parameters such as tobacco plant density, tensile modulus and Poisson 's ratio. Combined with relevant literature (*Zhang T. et al., 2018; Han M. et al., 2024; Zhang L., 2015*) and data collected in the field, the model parameters of tobacco plants were selected in Table 1.

Table 1

Tobacco plant material parameters

Density (Kg·mm^{-3})	Tensile modulus (N·mm^{-2})	Poisson's ratio
4.5E-0.7	1.1E+0.4	0.33

In order to accurately reflect the change rule of the flexible connection force between tobacco stems and tobacco leaves, it is necessary to add a fixed connection between tobacco stems and the earth to make it unable to move in any direction when analyzing the falling conditions of tobacco leaves in tobacco.

The connection between tobacco stems and leaves is modeled using a bushing force. Due to the numerous and complex parameters involved in flexible sleeve connections, there is currently limited literature and few relevant case studies available. Therefore, based on previously measured physical and chemical properties, as well as the shedding force of tobacco plants in the early stage (*Qu Z. et al., 2024; Zhang H. et al., 2022*), the parameters for the flexible sleeve force were defined as shown in Table 2. The central point at the junction between the tobacco stem and leaf was selected as the connection point for applying the flexible bushing force, labeled Bushing1.

Table 2

Flexible connection sleeve force parameters

Connection force	Translation characteristics (x, y, z)		Rotation characteristics (x,y,z)		remark
	stiffness coefficient (N·mm)	damping coefficient (N·s·mm^{-1})	stiffness coefficient (N·mm/deg)	damping coefficient (N·mm·s/deg)	
Bushing 1	1.8	10	30	100	Connection between tobacco stem and leaf

Step function was used to apply increasing external load to tobacco leaves in ADAMS software, and the separation conditions of tobacco stems and leaves were analyzed. By referring to the relevant literature (*Wen, B., 2010*) and combining with the fracture force of tobacco petiole measured above, the external load range was set to 5-50 N, and the direction of external load was set along the negative direction of Y axis. The initial external load was set to 5 N, and then 10 N was added every 1 second. The functional equation is written as: + 5 + STEP (time, 1, 0, 1.01, 5) + STEP (time, 2, 0, 2.01, 10) + STEP (time, 3, 0, 3.01, 10) + STEP (time, 4, 4, 0, 4.01, 10) + STEP (time, 5, 0, 5.01, 10). The simulation time is set to simulate the falling process of tobacco leaf.

RESULTS AND DISCUSSIONS

Simulation Results Analysis

Figure 10 shows the velocity and acceleration curves of tobacco leaves in the X direction when subjected to external forces. As shown in the figure, since the tobacco leaves are only subjected to external loads in the negative Y direction, there is almost no velocity in the X direction, and the acceleration is also zero between 0s and 2 s. This indicates that when the external load is between 5 N and 15 N, the connection force (Bushing1) between the tobacco leaves and the tobacco stalk has not reached the breaking point. After 2 s, when the external load suddenly increases to 25 N, there is a significant change in velocity in the X direction, and the acceleration is no longer zero. This is because when the connection force reaches the breaking limit and the external load continues to increase, Bushing1 needs to transfer the received energy through lateral vibration. This shows that when the external force reaches 25 N, it has met the breaking condition of Bushing1.

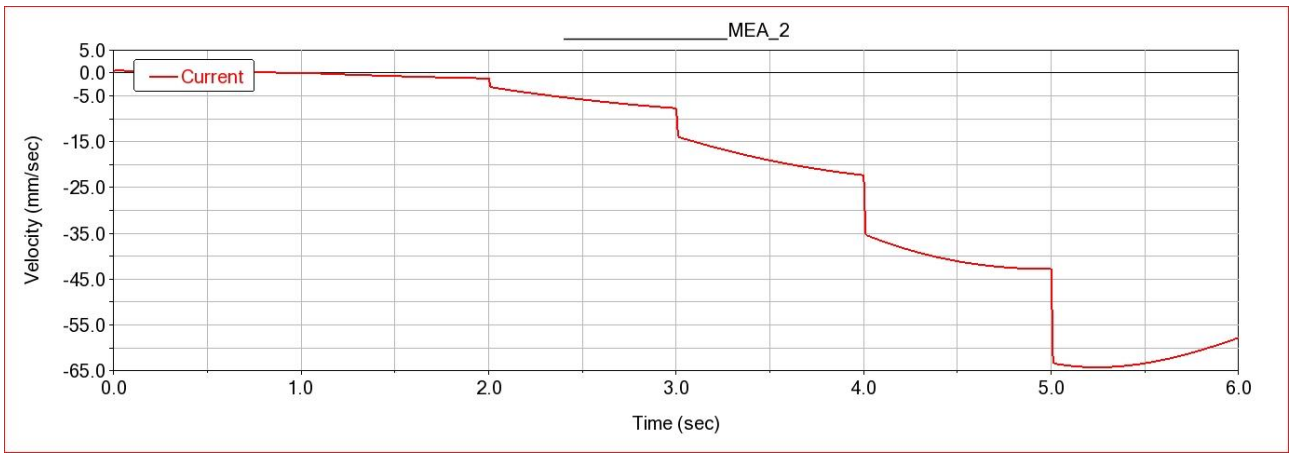

(a) X axis speed change curve of leaf

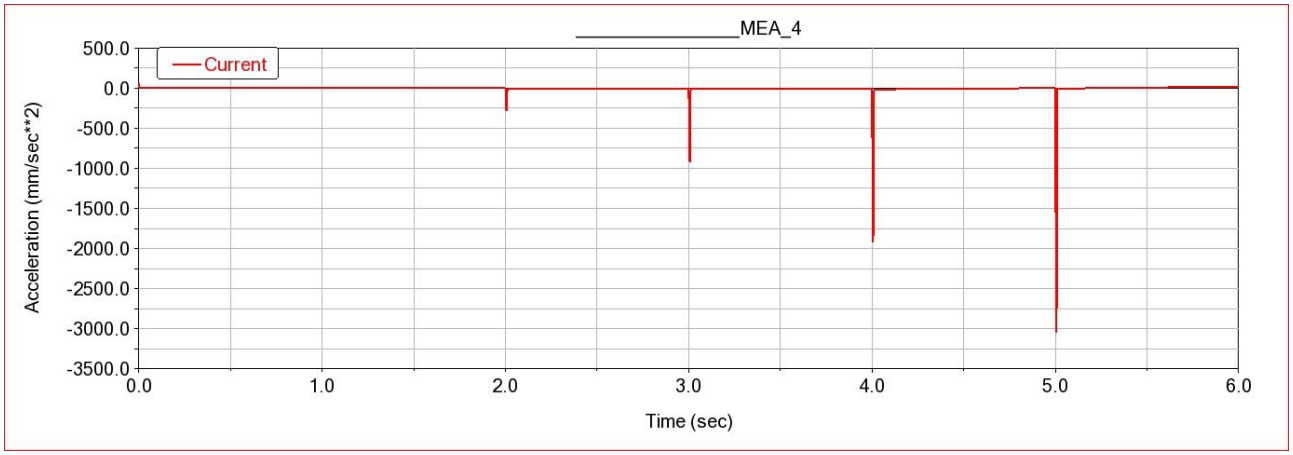

(b) X axis acceleration curve of leaf

Fig. 10 - Curves of X-axis velocity and acceleration of tobacco leaf

The flexible connecting sleeve force Bushing1 between tobacco leaf and stem exceeded the bearing limit when the external force reached 25 N at the end of the second. Figure 11 illustrates the displacement curve of the flexible sleeve force. At the end of 2 seconds, the displacement of the Y axis reached 1.2981 mm. This indicates that the shedding condition for the tobacco leaf occurs when the Y-axis displacement of the flexible connection (Bushing1) reaches 1.2981 mm.

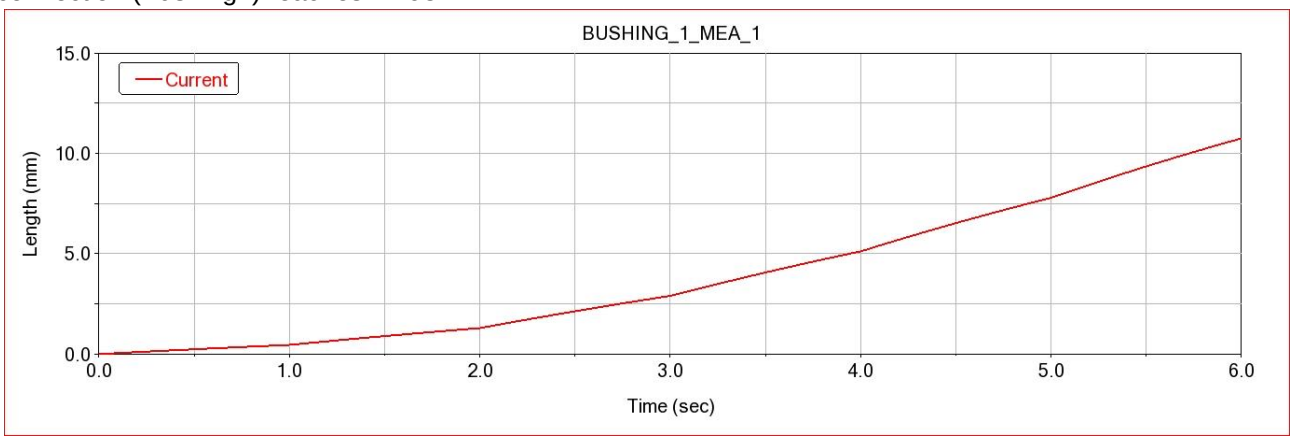

Fig. 11 - Flexible connection force displacement curve

Harvesting Process Simulation

The virtual prototype simulation analysis of the tobacco leaf picking process is to study the force change of the tobacco leaf during the picking process of the picking device, and to compare the force of the flexible picking mechanism and the rigid picking mechanism on the tobacco leaf. In this paper, the tobacco leaf picking device is taken as the research object. Because the picking process of a tobacco leaf is only affected by a picking rod, the number of picking rods is simplified to 1.

Import the model and set the material properties

The three-dimensional model of tobacco and picking rod is saved as "Parasoild" (*.x _ t) format, and then imported into ADAMS to construct the simulation picking system of tobacco plant-picking rod. The relative position of picking rod and tobacco stem is adjusted. The axis direction of tobacco stem coincides with the Y axis, the vein of tobacco leaf is parallel to the X-Y plane, and the picking rod is parallel to the Z axis and placed above the tobacco leaf. The materials of picking rod are steel and rubber respectively. The relevant performance parameters of steel and rubber (*Hou J. et al., 2022*) are shown in Table 3.

Table 3

Physical performance parameters of picking rod

Material type	Elastic modulus ($N \cdot mm^{-2}$)	Density ($Kg \cdot mm^{-3}$)	Poisson's ratio
Steel	2.06 E+05	7.85 E-06	0.3
Rubber	7.84	1.5 E-06	0.47

Adding Constraints, Drivers, and Sensors

Add constraints

The flexible connection between the two parts of the tobacco is still based on the data listed in Table 2. The picking rod is added with a negative moving pair relative to the earth along the Y axis, and the tobacco stem and the earth are fixed by a fixed pair.

Add driver

According to the previous calculation, when the rotation speed of the picking rod is 1.73 km/h ~ 5.08 km/h, the vertical downward combined speed is 0.865 km/h ~ 2.54 km/h, and the slip drive is added to the negative slip pair of the shaft to be 0.24 m/s, 0.4 m/s, 0.55 m/s and 0.71 m/s.

Define contact

The research on the contact parameters between tobacco and other materials in the literature is limited. Referring to the wood which is close to the physical and chemical properties of tobacco, combined with the relevant data measured above, and consulting the relevant references (*Jin C. et al., 2023*), the specific contact parameters are shown in Table 4.

Table 4

Contact parameters of different materials

Material type	Stiffness coefficient ($N \cdot mm^{-1}$)	Force index	Damping coefficient ($N \cdot s \cdot mm^{-1}$)	Static friction factor	Dynamic friction coefficient
Steel-Wood	2855	1.5	0.57	0.3	0.25
Rubber-Wood	2855	1.1	0.57	0.5	0.36

Define the sensor

Based on the previous analysis, Sensor1 is configured to monitor the displacement of the flexible connection bushing force (Bushing1) along the Y-axis. When the displacement exceeds 1.2981 mm, it is determined that the connection between the tobacco stem and leaf has fractured. At this point, both Sensor1 and Bushing1 are considered to have failed, indicating that the tobacco leaf has detached and fallen, completing the picking process. The sequence of the picking process is illustrated in Figure 12.

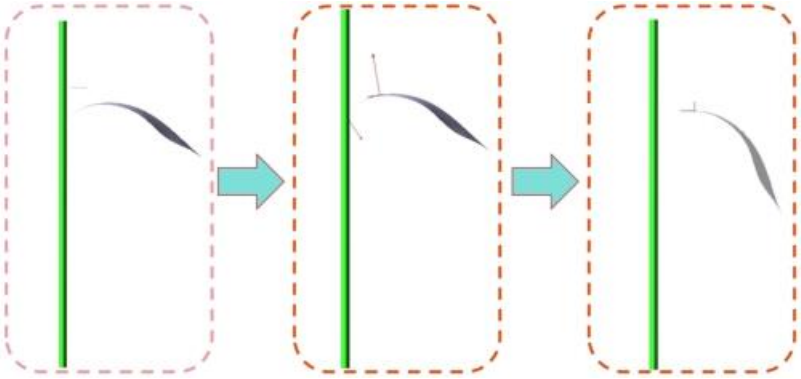

Fig.12 - Simulation of tobacco picking process

Simulation Results Analysis

The speed of the picking rod along the negative direction of the Y axis is 0.24 m/s, 0.4 m/s, 0.55 m/s, 0.71 m/s, respectively. As shown in Figures 13 ~ 16, the left side is the contact force change curve when the rigid picking rod collides with the tobacco leaf, and the right side is the contact force change curve when the flexible picking rod collides with the tobacco leaf.

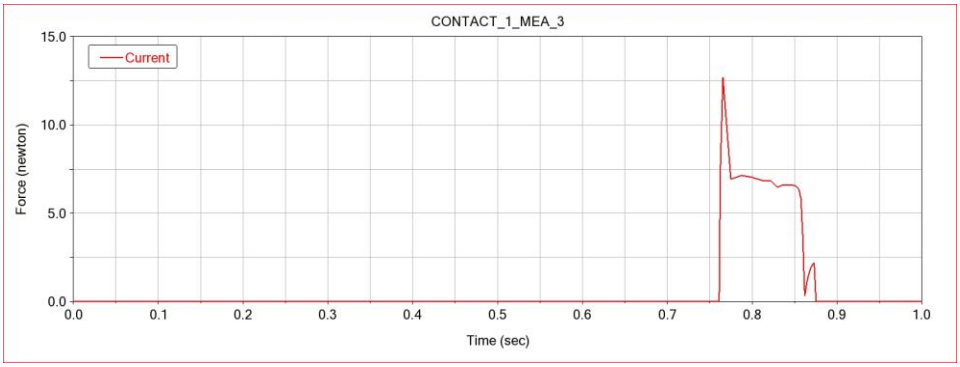

(**a**)

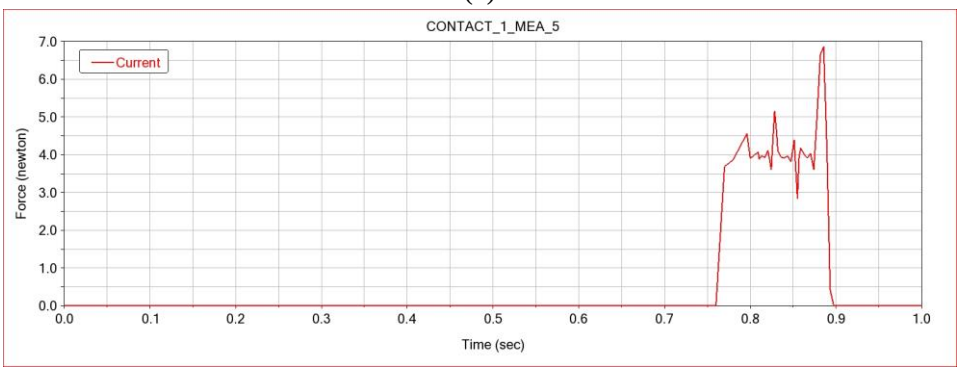

(**b**)

Fig. 13 - The collision force of tobacco leaves when the speed of picking rod is 0.24 m/s

(a) Rigid picking rod contact force; (b) Contact force of flexible picking rod

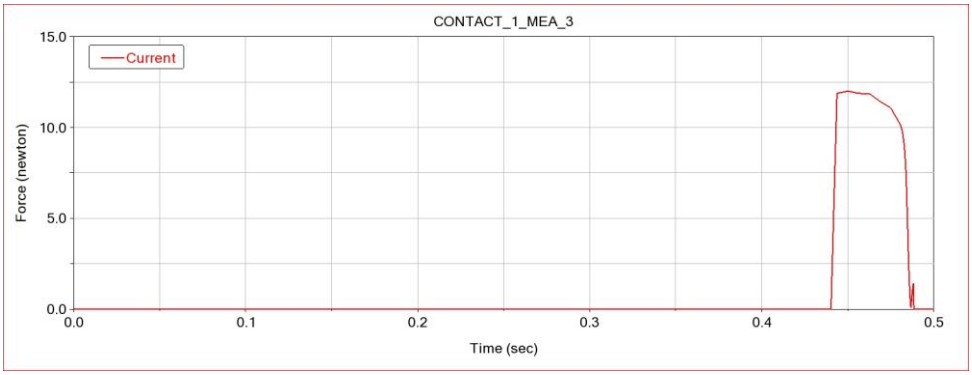

(**a**)

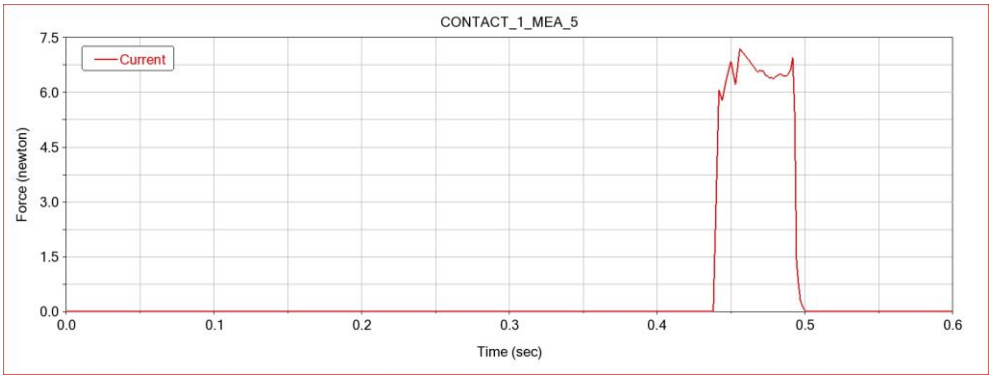

(**b**)

Fig. 14 - The collision force of tobacco leaves when the speed of picking rod is 0.4/s

(a) Rigid picking rod contact force; (b) Contact force of flexible picking rod

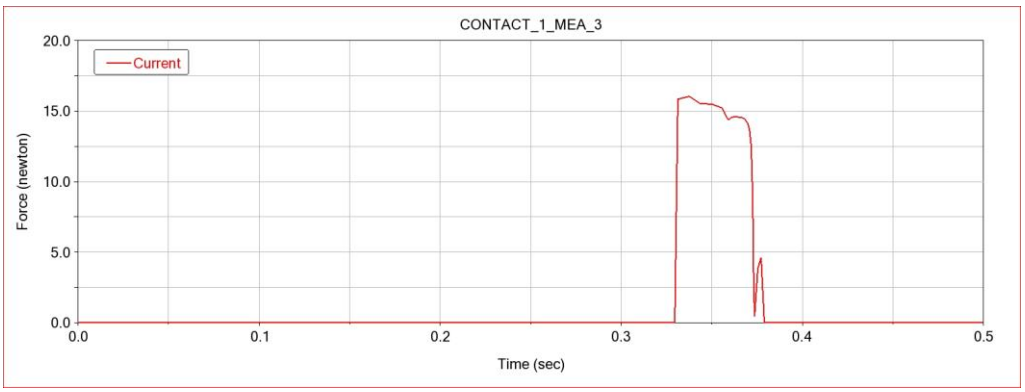

(**a**)

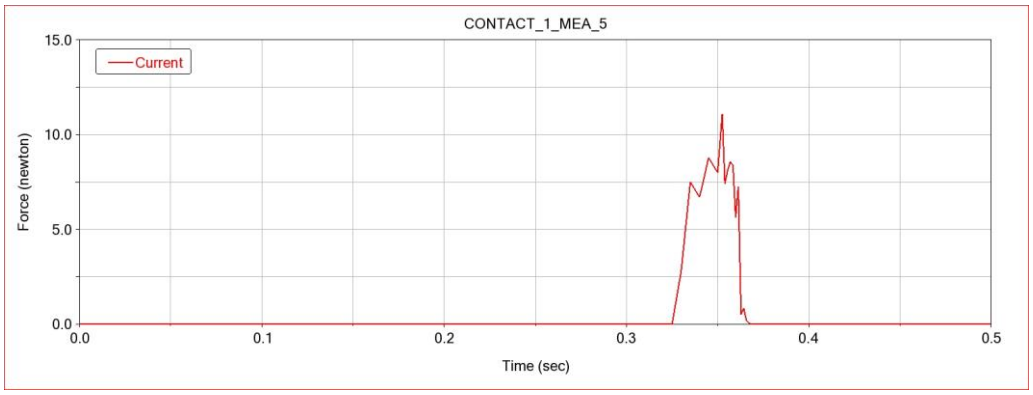

(**b**)

Figure .15 - Impact force on tobacco leaves when the speed of picking rod is 0.55 m/s

(a) Rigid picking rod contact force; (b) Contact force of flexible picking rod

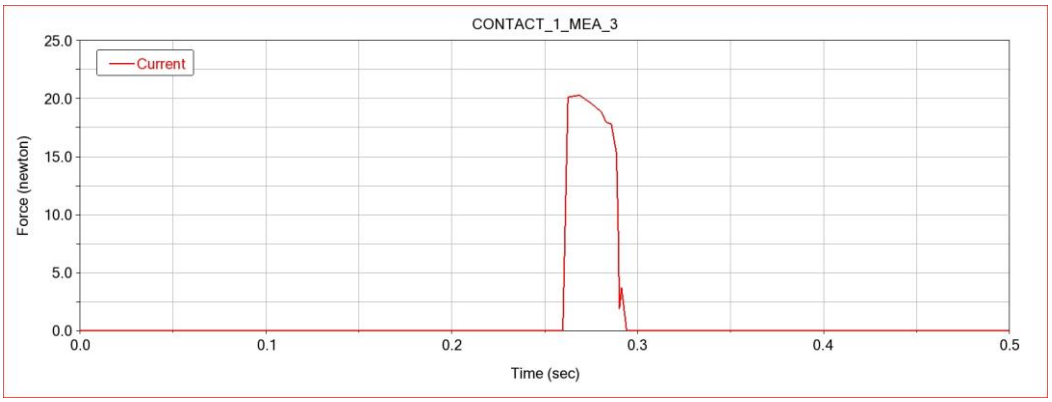

(**a**)

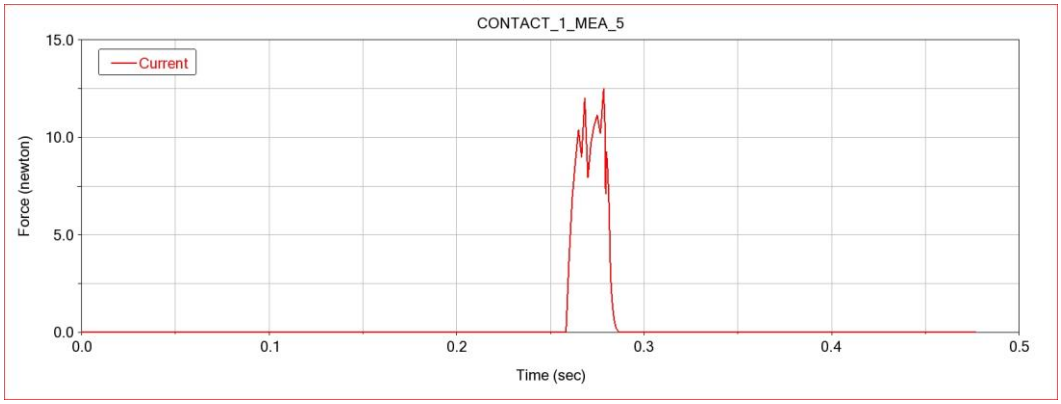

(**b**)

Fig. 16 - Impact force on tobacco leaves when the speed of picking rod is 0.71 m/s

(a) Rigid picking rod contact force; (b) Contact force of flexible picking rod

The comparative analysis of test data shows that:

By comparing the simulation test data on the left and right sides, it is found that the change rule of the overall curve of the two is similar, but it is relative to the rigidity. For the picking rod, the action time of the flexible rubber picking rod on the tobacco leaves is prolonged, and the effect of reducing the collision force is obvious.

Comparing the four groups of different picking rod speeds, it is found that when the picking rod speed is 0.4 m/s, the corresponding flexible picking rod collision force in Figure 16(b) is the smallest.

In summary, combined with the comprehensive consideration of tobacco picking efficiency and collision damage, when the vertical speed of the picking rod is 0.4 m/s, the picking effect of the flexible rubber picking rod is the best.

Field Trials

Test Conditions and Equipment

The field experiment was conducted in a tobacco field located in Xuchang, Henan Province, focusing on the harvesting of middle-position tobacco leaves. The experimental setup is illustrated in Figure 17. The instruments and equipment used included the custom-built tobacco leaf bionic picking machine, a computer, and a high-speed camera system. This experiment was performed outdoors. During the trials, trained operators operated the bionic picking machine, adjusting its forward operating speed to perform straight-line picking operations under varying conditions.

Fig. 17 - Field experiment plot

Experimental Design

The test materials and contents are shown in Table 5. According to the working principle analysis and pre-experimental analysis of the tobacco simulation picking device, it is concluded that the rotation speed of the picking rod, the inclination angle of the picking plane, the spacing of the picking rod, and the material of the picking rod have a great influence on the efficiency and harvesting quality of the picking device. The damage rate and operating efficiency of tobacco leaves are selected as test indicators. Each test sample group consisted of two rows of tobacco plants, with a total length of approximately 150 m.

After each test group, the harvested tobacco leaves in the collection box were gathered for evaluation. Each leaf was examined to determine whether the main stem was broken and whether the area of leaf loss exceeded the predefined damage threshold. The classification criteria for harvested tobacco leaves are illustrated in Figure 18. The number of damaged and intact tobacco leaves was recorded separately, and the damage rate was calculated using the following formula.

Table 5

Tobacco plant material parameters

Project	Test equipment	Test site	Experiment variables	Test metrics
elements	The processed tobacco leaf bionic picking machine, computer and high-speed camera system.	Xu chang, Henan Provinc	The picking rod, the inclinatior angle of the picking table and the picking rod spacing	The damage rate and operation efficiency

Fig. 18 - Classified tobacco leaves

$$Z_s = \frac{W_s}{W_i + W_s} \times 100\% \quad (14)$$

where: Z_S is the leaf damage rate, %; W_S is number of damaged tobacco leaves; W_i is number of intact tobacco leaves.

According to the ADAMS simulation results, the picking effect of the picking rod with flexible rubber material is better than that of the steel picking rod. The test factors were determined to be the rotation speed of the picking rod, the inclination angle of the picking table and the picking rod spacing, which were expressed by A, B and C respectively. The damage rate and operation efficiency of the test index tobacco leaves were expressed by W_1 and W_2. The quadratic orthogonal rotation combination analysis method with three factors and three levels was used in the experiment. The factor coding was shown in Table 6, and a total of 17 groups were carried out. Design-Expert software was used to analyze the test results. The test results are shown in Table 7.

Table 6

Coding table of test factors

Codes	Factors		
	Picking rod speed A (m/s)	Picking table inclination B (°)	Picking pole spacing C (mm)
-1	0.6	25	80
0	0.8	30	90
1	1	35	100

Table 7

Test scheme and results

No.	Factors			W_1 Tobacco leaf breakage rate (%)	W_2 Operational efficiency (km/h)
	A Picking rod speed (m/s)	B Picking table inclination (°)	C Picking pole spacing (mm)		
1	0	1	1	25.94	2.360
2	0	-1	1	25.31	2.640
3	1	1	0	24.33	2.950
4	0	1	-1	25.11	2.380
5	-1	1	0	21.98	1.230
6	-1	0	0	23.34	1.562
7	1	0	0	24.54	3.130
8	0	0	0	18.34	2.505
9	-1	-1	0	21.64	1.638
10	1	0	-1	22.34	3.134
11	0	0	0	18.25	2.508
12	-1	0	-1	21.14	1.566
13	1	-1	0	22.84	3.280
14	0	-1	-1	24.74	2.620

No.	Factors			W_1 Tobacco leaf breakage rate (%)	W_2 Operational efficiency (km/h)
	A Picking rod speed (m/s)	B Picking table inclination (°)	C Picking pole spacing (mm)		
15	0	0	0	18.31	2.507
16	0	0	0	18.21	2.511
17	0	0	0	18.18	2.502

Experimental Results Analysis

The regression model of tobacco leaf breakage rate was established

The regression mathematical model of tobacco leaf damage rate W_1 was obtained by regression fitting of the test results:

$$W_1 = 18.26 + 0.74A + 0.35B + 0.73C + 0.29AB + 0.00AC + 0.065BC + 1.00A^2 + 3.44B^2 + 3.58C^2 \quad (15)$$

The determination coefficient of the regression equation is R2 = 0.9892, and the fitting degree is high. The regression model was analyzed by variance analysis, and the results are shown in Table 8.

Available: P < 0.0001 of the model, indicating that the regression equation is significant; a, C, A2, B2, C2 P < 0.01, the results were significantly affected; other factors and interaction terms P > 0.05, had no significant effect on the test index.

The significance of the influence of each factor on the damage rate of tobacco leaves is the rotation speed of the picking rod > the picking rod spacing > the inclination angle of the picking table. The interaction of each factor is shown in Figure 19.

Table 8

Test scheme and results Analysis of variance of tobacco leaf breakage rate

Source	Sum of Squares	df	Mean Squares	F Value	P Value
Model	127.65	9	14.18	71.20	<0.0001
A	4.43	1	4.43	22.22	0.0022
B	1.00	1	1.00	5.03	0.0599
C	4.20	1	4.20	21.11	0.0025
AB	0.33	1	0.33	1.66	0.2386
AC	0.000	1	0.000	0.000	1.0000
BC	0.017	1	0.017	0.085	0.7793
A^2	4.23	1	4.23	21.23	0.0025
B^2	49.75	1	49.75	249.75	<0.0001
C^2	53.96	1	53.96	270.88	<0.0001
Residual	1.39	7	0.20		
Lack of Fit	1.38	3	0.46	102.64	0.0003
Pure Error	0.018	4	4.470E-003		
Cor Total	129.04	16			

*Note: P<0.01 (extremely significant, **); p < 0.05 (significant, *)*

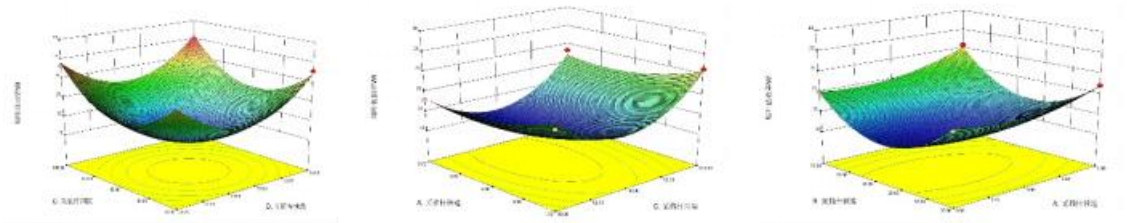

(a) (b) (c)

Fig. 19 - Effect of interaction of 21 factors on damage rate of tobacco leaf

(a) The interaction between the picking rod spacing and the inclination angle of the picking table;
(b) The interaction between the rotation speed of the picking rod and the picking rod spacing;
(c) The interaction between the rotation speed of the picking rod and the inclination angle of the picking table.

When the rotation speed of the picking rod is fixed, the effect of the interaction between the picking rod spacing and the inclination angle of the picking table on the damage rate of tobacco leaves is shown in figure 19(a). When the interval of the picking table is fixed, the inclination angle of the picking table is too large or too small, it will lead to the increase of the damage rate of tobacco leaves. When the inclination angle of the picking table is constant, the damage rate of tobacco leaves increases with the increase of the picking rod spacing.

When the inclination angle of the picking rod is fixed, the influence of the interaction between the picking rod spacing and the rotation speed of the picking table on the damage rate of the tobacco leaf is shown in Figure 18(b). When the picking rod spacing is constant, the damage rate of tobacco leaves increases with the increase of the rotation speed of the picking rod. When the picking rod speed is constant, the damage rate increases slowly with the increase of the picking rod spacing.

When the picking rod spacing has a fixed value, the effect of the interaction between the inclination of the picking table and the rotation speed of the picking rod on the damage rate of tobacco leaves is shown in figure 18(c). When the rotation speed of the picking rod is constant, the inclination angle of the picking table is too large or too small, which leads to the increase of the damage rate of tobacco leaves. When the inclination angle of the picking table is constant, the damage rate of tobacco leaves increases slowly with the increase of the rotation speed of the picking rod.

Establishment of a regression model for working efficiency

The regression mathematical model of working efficiency W2 is obtained by regression fitting of the test results:

$$W_2 = 2.51 + 0.81A - 0.16B - 0.001C + 0.019AB + 0.0001AC - 0.01BC - 0.19A^2 - 0.04B^2 + 0.033C^2 \quad (16)$$

The coefficient of determination for the regression equation was R2 = 0.9978, indicating an excellent degree of fit. The regression model was evaluated using analysis of variance, with the results presented in Table 9. The model's P-value was less than 0.0001, confirming its statistical significance. The quadratic terms of variables A, B and A2 had P-values less than 0.01, indicating a significant influence on the results. Additionally, B2 had a P-value less than 0.05, suggesting it also had a significant effect on the response variable. Other factors and interaction terms had P-values greater than 0.05, indicating no significant effect on the test indices. The ranking of the factors based on their influence on operational efficiency was as follows: picking rod speed > picking table inclination > picking rod spacing. The interaction effects among these factors are illustrated in Figure 20.

Table 9

Analysis of variance of operation efficiency

Source	Sum of Squares	df	Mean Squares	F Value	P Value
Model	5.65	9	0.63	354.73	<0.0001
A	5.28	1	5.28	2984.76	<0.0001
B	0.20	1	0.20	111.87	<0.0001
C	8.000E-006	1	8.000E-006	4.524E-003	0.9483
AB	1.521E-003	1	1.521E-003	0.86	0.3846
AC	0.000	1	0.000	0.000	1.000
BC	4.000E-004	1	4.000E-004	0.23	0.6488
A2	0.16	1	0.16	87.82	<0.0001
B2	6.754E-003	1	6.754E-003	3.82	0.0916
C2	4.711E-003	1	4.711E-003	2.66	0.1466
Residual	0.012	7	1.768E-003		
Lack of Fit	0.012	3	4.111E-003	363.81	<0.0001
Pure Error	4.520E-005	4	1.130E-005		
Cor Total	5.66	16			

*Note: P<0.01 (extremely significant, **); p < 0.05 (significant, *)*

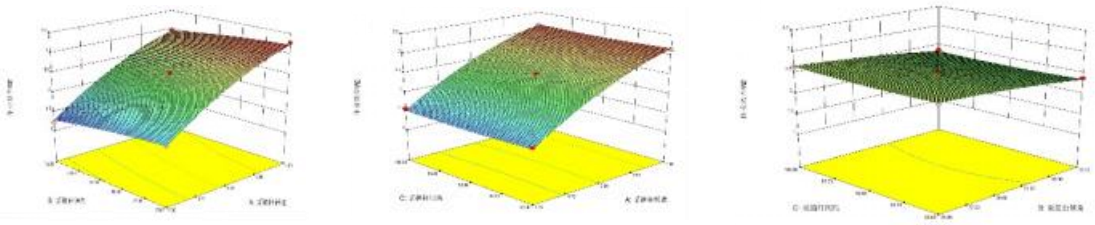

(a) (b) (c)

Fig. 20 - The effect of factor interaction on work efficiency

(a) The interaction between the rotation speed of the picking rod and the inclination angle of the picking platform;
(b) The interaction between the rotation speed of the picking rod and the picking rod spacing;
(c) The interaction between the inclination angle of the picking platform and the picking rod spacing.

When the picking rod spacing is a fixed value, the effect of the interaction between the picking rod speed and the inclination angle of the picking table on the operating efficiency is shown in Figure 20(a). When the inclination angle of the picking table is constant, with the increase of the rotation speed of the picking rod, the working efficiency gradually increases, and the change is more obvious. When the rotation speed of the picking rod is constant, the working efficiency increases with the decrease of the inclination angle of the picking table.

When the inclination angle of the picking table is fixed, the influence of the interaction between the picking rod speed and the picking rod spacing on the working efficiency is shown in Figure 20(b). When the picking rod speed is constant, the operating efficiency increases slightly with the decrease of the picking rod spacing, and the change is not obvious. When the picking rod spacing is constant, the working efficiency gradually increases with the increase of the rotation speed of the picking rod.

When the picking rod speed is constant, the influence of the interaction between the inclination angle of the picking table and the picking rod spacing on the working efficiency is shown in Figure 20(c). When the picking rod spacing is constant, the working efficiency gradually increases with the decrease of the inclination angle of the picking table. When the inclination angle of the picking platform is constant, the working efficiency increases slightly with the decrease of the picking rod spacing, and the change is not obvious.

In order to achieve better picking effect, the optimization module is used to optimize the regression model. By analyzing the constraints, the optimal parameter combination is obtained in the optimal combination of multiple parameters: picking rod speed 0.8 m/s, picking table angle 30°, picking rod spacing 90 mm, the tobacco leaf damage rate is 18.35%, the operation efficiency is 2.51 km/h, and the test index effect is the best.

The optimized parameter combination was tested and verified. The rotation speed of the picking rod was set to be 0.8 m/s, the inclination angle of the picking table was 30°, and the picking rod spacing was 90 mm. The average value of multiple tests was obtained. The damage rate of tobacco leaves was 18.32%, and the operating efficiency was 2.483 km/h, which verified the reliability of the model.

CONCLUSIONS

(1) To address the issues of low efficiency and high damage rates in the current tobacco harvesting process, the rotation speed of the picking rod, the dimensions of the picking frame, and the angle of the holding device were theoretically calculated and analyzed. Based on this analysis, a bionic tobacco leaf harvesting device was designed. The proposed device significantly enhances harvesting efficiency while effectively reducing the damage rate associated with mechanical picking.

(2) The tobacco leaf picking process was simulated using ADAMS software, focusing on analyzing the contact forces between rigid and flexible picking rods at different speeds. The optimal combination was identified as a vertical speed of 0.4 m/s using a flexible picking rod.

(3) Preliminary processing of the bionic harvester was completed, followed by field experiments to evaluate its performance. Design-Expert software was used to optimize and analyze the experimental data. The optimal combination of parameters for each experimental factor was determined as follows: the rotation speed of the picking rod was 0.8 m/s, the inclination angle of the picking table was 30°, and the picking rod spacing was 90 mm. Under these conditions, the tobacco leaf damage rate was 18.35%, and the operational efficiency reached 2.51 km/h.

(4) Using the optimized parameter combination, a follow-up harvesting test was conducted. The tobacco leaf breakage rate was 18.32%, with a relative error of only 0.1% compared to the predicted value. The operational efficiency reached 2.483 km/h, with a prediction error of 0.11%. These results confirm the reliability

of the optimized model. This study successfully achieved low-damage mechanized harvesting of tobacco leaves and provides a valuable reference for the development of bionic tobacco leaf harvesters designed to minimize leaf damage.

(5) The current harvesting equipment and experimental program are still in the preliminary stages of development, and the cost of the designed harvesting device remains relatively high. Future research will focus on investigating the effects of tobacco leaf surface properties on harvesting efficiency, with the aim of further optimizing the structural design to improve cost-effectiveness. Additionally, integration of a harvesting quality inspection system is planned to ensure consistent and reliable performance in real-world applications.

ACKNOWLEDGEMENT

This work is supported by Henan Provincial Science and Technology Research Project (222102110457, 242102111173); Henan Tobacco Company Science and Technology Special (2023410000240029, PYKJ202204); Henan Provincial Postdoctoral Funding Project (279456); China National Tobacco Corporation Tobacco Agricultural Machinery Research Project (110202301010); The Key Scientific and Technological Project of Henan Province Department of China (232102211087); Henan Province Science and Technology Research and Development Plan Joint Fund Project (232103810020).

REFERENCES

[1] Chen, M.Z.; Cheng, X.P.; Jia, X.D.; Zhang, L.P.; Li, Q.Y. (2018). Optimization of operating parameter and structure for corn ear picking device by bionic breaking ear hand. *Transactions of the Chinese Society of Agricultural Engineering (Transactions of the CSAE)*. 34(5): 15-22. DOI.10.11975/j.issn.1002-6819.2018.05.003

[2] Du, C.; Fang, W.; Han, D. (2024). Design and experimental study of a biomimetic pod-pepper-picking drum based on multi-finger collaboration. *Agriculture*. 14(2): 314.DOI.org/10.3390/agriculture14020314

[3] Du, Z.; Hu, Y.; Lu, Y. (2021). Design of structural parameters of cutters for tea harvest based on biomimetic methodology. *Applied Bionics and Biomechanics.* 2021(1): 8798299. DOI: 10.1155/2021/8798299

[4] Gao, J.; Zhang, F.; Zhang, J. (2022). Development and evaluation of a pneumatic finger-like end-effector for cherry tomato harvesting robot in greenhouse. *Computers and Electronics in Agriculture*. 197: 106879. DOI.org/10.1016/j.compag.2022.106879

[5] Gao, J.; Zhang, F.; Zhang, J. (2024). Picking patterns evaluation for cherry tomato robotic harvesting end-effector design. *Biosystems Engineering*. 239: 1-12. DOI.org/10.1016/j.biosystemseng.2024.01.009

[6] Gan, W.G.; Liang, W.; Yang, J.A. (2022). Tobacco leaf harvesting device.CN207604219U, 2018-07-13.

[7] Guo, T.; Zheng, Y.; Bo, W. Research on the Bionic Flexible End-Effector Based on Tomato Harvesting. *Journal of Sensors.* 2022(1): 2564952. DOI.org/10.1155/2022/2564952

[8] Han, M.; Li, M.; Duan, H. (2024). Rigid-flexible coupling simulation and experiment of plant stem clamping device based on ADAMS. *Transactions of the Chinese Society for Agricultural Machinery*. 55(02):109-117. DOI: 10.6041/j.issn.1000-1298.2024.02.010

[9] He, Z.; Ma, L.; Wang, Y. (2022). Double-Arm cooperation and implementing for harvesting kiwifruit. *Agriculture*. 12(11): 1763. DOI.org/10.3390/agriculture12111763

[10] Hou, J.; Xei, F.; Wang, X. (2022). Measurement of contact physical parameters of flexible rice straw and discrete element simulation calibration. *Acta Agriculturae Universitatis Jiangxiensis*. 44(03):747-758. DOI.org/10.13836/j.jjau.2022074

[11] Hou, Z.; Li, Z.; Fadiji, T. (2021). Soft gras mechanism of human fingers for tomato-picking bionic robots. *Computers and Electronics in Agriculture.* 182: 106010. DOI.org/10.1016/j.compag.2021.106010

[12] Jin, C.; Qi, Y.; Liu, G. (2022). Mechanism analysis and parameter optimization of soybean combine harvester reel. *Transactions of the Chinese Society for Agricultural Machinery*. 2023, 54(06):104-113. DOI: 10.6041/j.issn.1000-1298.2023.06.011

[13] Kurbah, F.; Marwein, S.; Marngar, T. Design and development of the pineapple harvesting robotic gripper. *Communication and Control for Robotic Systems*. 437-454. DOI.org/10.1063/5.0099837

[14] Li, X.; Zhang, W.; Xu, S. (2023). Low-damage corn threshing technology and corn threshing devices: A review of recent developments. *Agriculture*. 13(5): 1006. DOI.org/10.3390/agriculture13051006

[15] Liu, J.; Ma, W.K. (2012). Design and simulation of tobacco harvesting system based on virtual manufacturing technology. *Key Engineering Materials*. 522: 736-739. DOI.org/10.4028/www.scientific.net/KEM.522.736

[16] Luo, Y.; Li, J.; Yao, B. (2024). Research progress and development trend of bionic harvesting technology. *Computers and Electronics in Agriculture*. 222: 109013. DOI.org/10.1016/j.compag.2024.109013

[17] Li, Z.G. (2016). Design and Development of a Self-Propelled Intelligent Bionic Tobacco Leaf Harvesting System [D]. *Henan Agricultural University*, 2016. DOI: 10.27117/d.cnki.ghenu.2016.000055.

[18] Malekzadeh, M.S.; Queißer, J.F.; Steil, J.J. (2019). Multi-level control architecture for Bionic Handling Assistant robot augmented by learning from demonstration for apple-picking. *Advanced Robotics*. 33(9): 469-485. DOI:10.1080/01691864.2019.1587313

[19] Nie, Y.C.; Chen, Y. (2022). Measurement of new shoot parameters and mechanical property analysis of plucking fingers for high-quality green tea. *Manuf. Autom*. 2022, 44: 83-86.

[20] Papusha, S.K.; Kozhura, F.A.; Zhadko, V.V. (2021). Mechanization of tobacco harvesting. The state, problems and prospects of development. AIP Conference Proceedings. *AIP Publishing*. 2503(1): 030045. DOI:10.1063/5.0099837

[21] Sun, C.; Tan, S.; Sun, S. (2024). Design and test of the key components for a combing-type tobacco harvester. *International Journal of Agricultural and Biological Engineering.* 17(1): 145-153. DOI : 10.25165/j.ijabe.20241701.8324

[22] Wang, M.; Yan, B.; Zhang, S. (2022). Development of a novel biomimetic mechanical hand based on physical characteristics of apples. *Agriculture*. 12(11): 1871. DOI.org/10.3390/agriculture12111871

[23] Wen, B. (2010). Mechanical Design Manual, 5th ed.; *China Machine Press*: Beijing, China.

[24] Xu, W.T.; Zhao, J.; Cui, X.; Li, Q.Y.; Jin, C.Q. (2018). The bionics design and analysis on device of corn picking with dragging and cutting stem. *Journal of Agricultural Mechanization Research.* 40(07): 81-86. DOI: 10.13427/j.cnki.njyi.2018.07.015.

[25] Yu, J.; Chu, J.; Li, Y. (2020). Simulation Analysis on Key Mechanisms of the Automatic Tobacco Harvester Based on ADAMS. Recent Advances in Mechanisms, Transmissions and Applications: Proceedings of the Fifth MeTrApp Conference. *Springer Singapore*. 113-122. DOI.org/10.1007/978-981-15-0142-5_12

[26] Zhang, H.; Chen, B.; Hu, J. (2024). Comparative experiment of fresh corn ear picking devices based on collision characteristics. *Journal of Henan Agricultural University*. 58(01):87-95. DOI: 10.16445/j.cnki.1000-2340.20231127.002.

[27] Zhang, H.; Chen, B.; Li, Z. (2022). Design and simulation analysis of a reverse flexible harvesting device for fresh corn. *Agriculture*. 12(11):1953. DOI.org/10.3390/agriculture12111953

[28] Zhang, L.P.; Li, Q.Y. (2015). Speed of bionic breaking corn ear hand and experiment on power consumption. *Transactions of the Chinese Society of Agricultural Engineering (Transactions of the CSAE)*. 31(19): 9-14. DOI: 10.11975/j.issn.1002-6819.2015.19.002

[29] Zhang, T.; Liu, F.; Zhao, M. (2018). Determination of corn stalk contact parameters and calibration of Discrete Element Method simulation. *Journal of China Agricultural University*. 23(04): 120-127.

[30] Zhang, L. (2015). Theoretical Analysis and Simulation Research on Novel Bionic Corn-ear Snapping Mechanism. *Jilin University*.

[31] Zhu, H.J.; Wang, Z.M.; Bai, W.; Hu, G. (2014). Design of floating picking platform for tobacco leaf harvester. *Journal of Mechanical Research and Application*. 27(04):140-141. DOI: 10.16576/j.cnki.1007-4414.2014.04.074.